

Joint SAR imaging and wireless communication using the FBMC chirp waveform

Kehong ZHU^{1,2,3}, Jie WANG⁴, Xingdong LIANG^{1,2,3*}, Longyong CHEN^{1,2,3},
Yanlei LI^{1,2,3}, Xiangxi BU^{1,2,3} & Yirong WU^{1,2,3}

¹*Institute of Electronics, Chinese Academy of Sciences, Beijing 100190, China;*

²*National Key Laboratory of Science and Technology on Microwave Imaging, Beijing 100190, China;*

³*University of Chinese Academy of Sciences, Beijing 100049, China;*

⁴*College of Electronic and Information Engineering,
Nanjing University of Information Science & Technology, Nanjing 210044, China*

Received 29 December 2018/Revised 4 March 2019/Accepted 15 March 2019/Published online 24 September 2019

Citation Zhu K H, Wang J, Liang X D, et al. Joint SAR imaging and wireless communication using the FBMC chirp waveform. *Sci China Inf Sci*, 2020, 63(4): 149302, <https://doi.org/10.1007/s11432-018-9830-1>

Dear editor,

Joint system designs help improve resource efficiency and reduce the volume and energy consumption of electronic systems; therefore, such joint systems have become a research hot spot in recent years [1, 2]. To improve the flexibility of the working modes and to enhance adaptability to complex applications, joint synthetic aperture radar (SAR) and communication is recommended. Orthogonal frequency division multiplexing (OFDM) [3] waveforms have been widely studied in joint radar and communication systems because they have high spectral efficiency, flexible subcarrier modulation, and easy implementation [1, 4]. Nevertheless, to prevent multipath interference, the cyclic prefix (CP) set by OFDM produces false targets in the SAR image and reduces the spectral efficiency [2, 4]. Besides, its high amplitude of subcarrier sidelobes lead to severe inter-subcarrier interference [4]. The filter bank multicarrier (FBMC) [5] is a multicarrier waveform similar to OFDM; therefore, it also has the abovementioned advantages. In addition, the subcarrier sidelobes amplitude of the FBMC become extremely low when the prototype filter is used; this reduces the inter-subcarrier interference. FBMC does not use CP to combat inter-symbol

interference and inter-carrier interference, which avoids the false targets in imaging and improves the spectral efficiency [2, 4]. Therefore, FBMC waveforms have better performance in joint SAR and communication systems [2]. However, the integral sidelobe ratio (ISLR) of the conventional FBMC waveform is very high, which causes problems such as weak targets being masked by strong targets.

In this study, transmission information and chirp signals are simultaneously modulated into the FBMC symbols to form an FBMC chirp waveform. The waveform proposed in our research has two main advantages over the conventional FBMC waveform. First, the FBMC chirp waveform has good imaging performance even while carrying a large amount of information. Second, by using the known chirp signal, complex channel estimation can be performed during demodulation; this avoids the real orthogonal requirement in the FBMC waveform channel estimation.

Preliminaries. The flight platform transmits a joint FBMC waveform to the ground with both the sensing and transmission functions. To avoid interference between the subcarriers and to keep the data rate the same as that of OFDM, the FBMC uses offset quadrature amplitude modulation [5].

* Corresponding author (email: xdliang@mail.ie.ac.cn)

The transmitted signal is

$$s(t) = \sum_{n=0}^{N-1} \sum_{m=0}^{M-1} a_{m,n} g_{m,n}(t), \quad (1)$$

where N is the number of even real symbols; M is the number of subcarriers; and $a_{m,n}$ is the transmitted real-valued symbol obtained by taking the real and imaginary parts of the 2^{2K} -QAM data. The filter bank $g_{m,n}(t)$ can be expressed as

$$g_{m,n}(t) = g(t - n\tau_0) e^{j2\pi m \Delta f t} e^{j\frac{\pi}{2}(m+n)}, \quad (2)$$

where $g(t)$ is the prototype pulse; τ_0 is the time offset between the real and imaginary parts (equal to half the symbol duration T); Δf is the subcarrier frequency interval; and $\tau_0 = T/2 = 1/(2\Delta f)$.

Modulation of the FBMC chirp waveform. By converting (1) to the frequency domain, we obtain

$$S(f) = \sum_{n=0}^{N-1} \sum_{m=0}^{M-1} a_{m,n} G(f - m\Delta f) \cdot e^{j\phi}, \quad (3)$$

where $G(f)$ is the prototype filter in the frequency domain, and $\phi = -2\pi f n \tau_0 + \frac{\pi}{2}(m+n)$ is the phase. By sampling the transmitted signal at $1/T$ intervals (i.e., $f = m\Delta f$), we obtain the following data of the subcarriers:

$$S(m\Delta f) = \sum_{n=0}^{N-1} \sum_{m=0}^{M-1} a_{m,n} \delta(f - m\Delta f) \cdot e^{j\phi}. \quad (4)$$

Here, $\phi = \frac{\pi}{2}(m+n-2mn)$ is the phase of the subcarriers; this phase interleaves the subcarrier data real and imaginary parts [5]. In the FBMC chirp modulation, the transmission information is encoded into the first $N-2$ symbols, and the chirp signal is compensated in the real and imaginary parts by using the last two symbols. The encoding information of the last two auxiliary symbols is designed as follows:

$$\begin{aligned} a_{m_e, N-2} &= (-1)^{m_e N - \frac{5m_e + N-2}{2}} \cdot \Re\{K(m_e)\}, \\ a_{m_o, N-2} &= (-1)^{m_o N - \frac{5m_o + N-3}{2}} \cdot \Im\{K(m_o)\}, \\ a_{m_e, N-1} &= (-1)^{m_e N - \frac{3m_e + N-2}{2}} \cdot \Im\{K(m_e)\}, \\ a_{m_o, N-1} &= (-1)^{m_o N - \frac{3m_o + N-1}{2}} \cdot \Re\{K(m_o)\}, \end{aligned} \quad (5)$$

where m_e and m_o are the even and odd subcarriers, respectively; $\Re\{\cdot\}$ and $\Im\{\cdot\}$ are the real and imaginary parts, respectively. $K(m) = \exp(j\pi(m\Delta f)^2/k) - \sum_{n=0}^{N-3} a_{m,n} e^{j\frac{\pi}{2}(m+n-2mn)}$, where k is the chirp rate. By substituting (5) into (4), we obtain

$$S(f)|_{f=m\Delta f} = \exp(j\pi(m\Delta f)^2/k_r). \quad (6)$$

This shows that when using the proposed encoding method, the transmitted signal can be reconstructed into a chirp signal with good imaging capability.

Pre-demodulation of the FBMC chirp waveform. The echo can be expressed as follows:

$$S_r(f) = S(f) \cdot H(f), \quad (7)$$

where $H(f)$ are the channel effects. It is necessary to extract information on the corresponding subcarriers to reconstruct the chirp echoes. The following two restrictions must be met during the pre-demodulation.

(1) The echo sampling interval needs to be the same as the modulation interval, that is, $1/T$; otherwise, the channel cannot be described correctly.

(2) The length of the echo needs to be less than $(N/2 + 1)$ symbol duration. The sampled echo length was T . Its maximum unambiguous swath was $cT/2$, and the corresponding maximum echo length was $(N/2 + 1) \times T$. This echo length requirement can be met by digital beamforming for the receive technique [6].

Combining (6) and (7), the frequency domain signal can be expressed as

$$\begin{aligned} S_r(m\Delta f) &= S(f) \cdot H(f)|_{f=m\Delta f}, \\ &= \exp(j\pi f^2/k_r) \cdot H(f)|_{f=m\Delta f}. \end{aligned} \quad (8)$$

The corresponding time domain signal is

$$s_r(t_r) = \exp(j\pi k t^2) \otimes h(t)|_{t \leq T}. \quad (9)$$

The pre-demodulated signal can be described as a chirp echo of a channel whose maximum delay does not exceed T . Pre-demodulated signals can be imaged by conventional imaging algorithms, such as the range-Doppler algorithm [7].

Channel estimation method. With the pre-demodulated signal, it is possible to employ a conventional channel estimation algorithm. For example, by using the least squares estimation [8] and considering the influence of the noise n , the channel response can be obtained as

$$\hat{H}(f) = \frac{S_r(f)}{P(f)} = H(m\Delta f) + \frac{n}{P(m\Delta f)}, \quad (10)$$

where $P(f) = \exp(j\pi f^2/k)$ is the chirp signal.

Channel estimation has two main steps. (1) Pre-estimation. The channel response on the subcarriers is pre-estimated by using the conventional method. (2) Interpolation. The obtained pre-estimation results $\hat{H}(f_r)$ are interpolated to obtain the channel response \hat{H}_{m_0, n_0} of the entire pulse. The echo through the analysis filter bank is

$$Y_{m_0, n_0} = \langle s_r(t), \gamma_{m_0, n_0}(t) \rangle$$

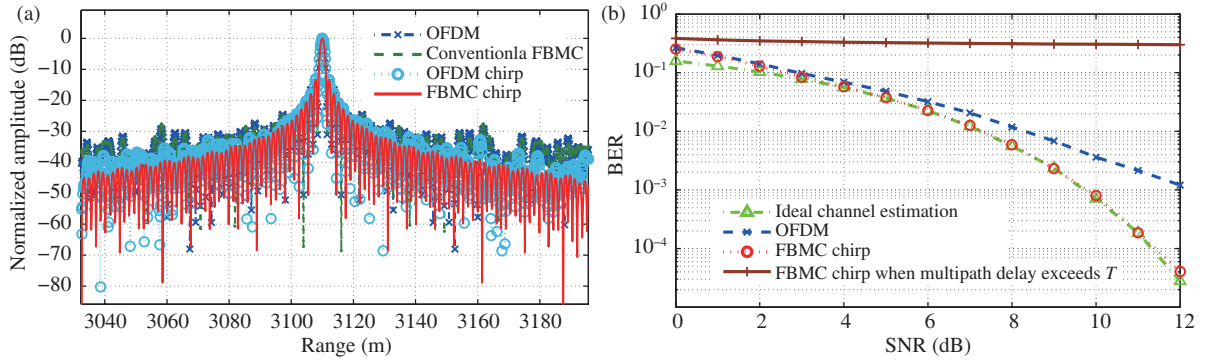


Figure 1 (Color online) Results of (a) imaging, (b) communication.

$$\begin{aligned}
 &= \sum_n \sum_m a_{m,n} H_{m,n} \langle g_{m,n}, \gamma_{m_0, n_0} \rangle \\
 &= \sum_n \sum_m a_{m,n} H_{m,n} \delta_{m, m_0} \delta_{n, n_0} (1 + jd) \\
 &= a_{m_0, n_0} H_{m_0, n_0} (1 + jd). \quad (11)
 \end{aligned}$$

The signal is equalized by using the channel estimation result, and the demodulated result can be obtained by taking the real part

$$\hat{a}_{m_0, n_0} = \Re \left\{ \frac{Y_{m_0, n_0}}{\hat{H}_{m_0, n_0}} \right\} \approx a_{m_0, n_0}. \quad (12)$$

Experimental results and analysis. In this research, an experimental pulse contained eight FBMC symbols. The first six symbols conveyed the transmission information, and the last two symbols modulated the chirp signal. The symbol duration was 40 μ s, the bandwidth was 100 MHz, the sampling rate was 120 MHz, the Doppler bandwidth was 100 Hz, and the PRF was 120 Hz. To evaluate the imaging performance, we performed range slicing of the OFDM, the conventional FBMC, and the OFDM and FBMC chirp waveforms [9]; the results are shown in Figure 1(a). Compared with the other three waveforms, the range sidelobes of the FBMC chirp waveform was significantly suppressed. Figure 1(b) shows the communication performance simulation. The green line is the relationship between the communication bit error rate (BER) and the signal-to-noise ratio (SNR) for the ideal channel estimation. The blue line shows the result of the OFDM waveform. Because the influence of non-orthogonal factors such as the Doppler shift, the channel estimation of the OFDM waveform was erroneous, which deteriorated the BER. The red line shows the result of the FBMC chirp waveform. As the SNR increases, the channel estimation performance improves, and the BER gradually approaches the ideal result. However, the brown line shows that

when the multipath delay exceeds the duration of one symbol, channel estimation errors will occur; this causes the BER to deteriorate dramatically.

Conclusion. We proposed the FBMC chirp waveform for solving the problem of poor pulse compression performance of the conventional FBMC waveform. By modulating the chirp signal into the FBMC symbols, high-quality imaging could be achieved while ensuring high-speed digital transmission. Furthermore, by using a known chirp signal, it was possible to perform channel estimation, which avoided the real orthogonality restriction of the conventional FBMC waveform. The simulation results show that the FBMC chirp waveform can improve the imaging quality as well as the accuracy of communication. Therefore, good performance can be achieved in the joint system.

References

- Han L, Wu K. Multifunctional transceiver for future intelligent transportation systems. *IEEE Trans Microwave Theory Tech*, 2011, 59: 1879–1892
- Zhu K H, Wang J, Liang X D, et al. Filter bank multicarrier waveform used for integrated SAR and communication systems. *J Radars*, 2018, 7: 602–612
- Nee R V, Prasad R. *OFDM for Wireless Multimedia Communications*. Norwood: Artech House, 2000
- Farhang-Boroujeny B. OFDM versus filter bank multicarrier. *IEEE Signal Process Mag*, 2011, 28: 92–112
- Bellanger M G. *FBMC physical layer: a primer*. PHYDYAS, 2010
- Gebert N, Krieger G, Moreira A. Digital beamforming on receive: techniques and optimization strategies for high-resolution wide-swath SAR imaging. *IEEE Trans Aerosp Electron Syst*, 2009, 45: 564–592
- Cumming I G, Wong F H. *Synthetic Aperture Radar Imaging: Algorithms and Implementation*. Beijing: Publishing House of Electronics Industry, 2012
- Qiao Y T, Yu S Y, Su P C, et al. Research on an iterative algorithm of LS channel estimation in MIMO OFDM systems. *IEEE Trans Broadcast*, 2005, 51: 149–153
- Wang J, Liang X D, Ding C B, et al. An improved OFDM chirp waveform used for MIMO SAR system. *Sci China Inf Sci*, 2014, 57: 062306